Gas Phase Lubrication Study with an Organic Friction Modifier

Jennifer Eickworth (jennifer.eickworth@iwm.fraunhofer.de)
Fraunhofer IWM MikroTribologie Centrum https://orcid.org/0000-0003-3206-5872

Jonas Wagner
Fraunhofer Institute for Mechanics of Materials IWM: Fraunhofer-Institut fur Werkstoffmechanik IWM

Philipp Daum
Fraunhofer IWM MikroTribologie Centrum

Martin Dienwiebel
Karlsruher Institut für Technologie: Karlsruher Institut fur Technologie

Thomas Rühle
BASF SE

Research Article

Keywords: laboratory tests, controllable atmosphere, tribometer, organic friction modifier

Posted Date: August 4th, 2021

DOI: https://doi.org/10.21203/rs.3.rs-751081/v1

Gas phase lubrication study with an organic friction modifier

J. Eickworth, J. Wagner, P. Daum, M. Dienwiebel, T. Rühle

Abstract

Friction modifier additive technologies play a crucial role in controlling friction and wear of lubricated tribological systems. Novel additives are usually evaluated using formulations of varying concentrations. It can be very difficult to understand the underlying mechanisms in those laboratory tests because of the interaction of base oil with the additives. It thus can be insightful to perform model experiments in a controllable atmosphere. This can be achieved for instance by integrating a tribometer into a vacuum system comprising in-situ surface analytical methods.

In this work, a nitrogen containing organic friction modifier is adsorbed from the gas phase onto a Fe_2O_3 surface. Different coating thicknesses are prepared by varying the duration of the vapor deposition, so that the influence of the coating thickness on the friction behavior can be investigated. The chemical composition of the coated surfaces is also analyzed by coupling to an XPS photoelectron spectrometer.

Contrary to the assumption that layers are formed, this friction modifier accumulates in droplets on the Fe_2O_3 surface. The number of droplets as well as the radii of droplets increase with evaporation time. The chemical composition of the additive does not change as a result of the gas phase deposition. In the friction tests, the smallest friction values are found for a very low coverage of droplets. For larger droplets, friction increases due to a capillary neck of additive that forms between the sliding surfaces and is dragged along during the friction test.

Using gas phase adsorption of a nitrogen containing organic friction modifier it was possible to establish a correlation between droplet morphology and the friction behavior.

---

1. Introduction

Friction modifier additives can be roughly divided into organic friction modifiers (OFM), functionalized polymers, soluble organo-molybdenum additives and dispersed nanoparticles [1]. Besides fatty acids, OFM's can comprise of carboxylates, alcohols, imides, borates, phosphorus compounds, ionic liquids, amides and amines [2].The adsorption mechanism and lubrication mechanisms of fatty acids was in the focus of numerous studies during the last century (e.g. [3–8]) and the friction reduction is often explained using the boundary lubrication model that goes back to Hardy in 1922 [9].Later, for some OFM's also a 'thick film' lubrication mechanism was observed that could not be well explained at the time [10, 11]. Moreover, as fatty acids can be corrosive and can cause damage, amines and their derivates are considered to offer a promising alternative. Therefore recently, research on OFM has triggered new interest and created new opportunities for the friction modifier additives market. The ongoing trend towards low-viscosity oils in order to reduce liquid friction losses increases the requirements especially for friction modifier additives, as friction must remain low even in the mixed lubrication regime. The adsorption behavior of amines has been reported in literature, but not to such extent as fatty acids. This lack of knowledge and more stringent environmental guidelines motivated us to seek a better understanding of the adsorption and mode of action of amine based friction modifiers.

During friction tests, complex reactions can occur in boundary lubrication between the contacting asperities and the additives. It can be very difficult to understand these mechanisms in an oil lubricated situation because of the interaction of base oil with the additives. It thus has been found insightful, to perform model experiments in a controllable atmosphere [12]. This can be achieved for instance by integrating a tribometer into a vacuum system comprising in-situ surface analytical methods, such as a photoelectron spectrometer (XPS), an Auger electron spectrometer (AES) or a secondary ion mass spectrometer (SIMS), allowing the surfaces to be investigated with respect to their chemical composition before and after the tribological experiments without contact to the atmosphere. Using an effusion cell or an electron beam evaporator allows to deposit molecularly thin lubricant or additive layers on a defined surface. Variable leak valves can also be used to change the partial pressure of a specific background gas in which the friction experiments take place. In the group of J. M. Martin, a so-called '*Environmental Controlled Analytical Tribometer* (ECAT)' was developed in the 1990s, which consists of a UHV chamber for tribological experiments, an XPS/AES system and a UHV preparation chamber (see e.g. in [12] and [13]). Similarly, in a subsequent works an home-built UHV microtribometer was developed that is coupled to the existing XPS system [14] and additionally installed an electron beam evaporator and an effusion cell for the deposition of organic layers.

Extensive work has been carried out over the last 30 years on the frictional properties of various model substances relevant to technical lubricants. The measurements were realized at the ECAT and often follow a similar pattern. A leak valve is used to control the partial pressure of the substances under investigation. The rubbing experiments are then carried out at controlled partial pressures, with a reference measurement in the liquid substance. XPS surface analysis is used to collect and evaluate additional information about the reaction mechanisms taking place. To date, studies with triethyl phosphite [15, 16], triethyl borate [17], phosphororganous compounds [18], and hexanthiol [12] are available. Another study by Rana et. al. investigated the influence of triethlyphosphates and -phosphites on the frictional behavior of oxidized Fe_3O_4 iron [19].

The correlation of measurements in vacuum and in liquid could be impressively shown by Martin et. al. in [20]. Microscopic images of a friction track after experiments in a controlled ethylphosphate atmosphere in the tribo-chamber (10 Pa) and in liquid show a similar morphology, so that it can be assumed that the friction mechanisms actually occurring in liquid-phase lubrication are well represented.

To our knowledge, all studies so far, have used model substances which do not have the same functional groups as common friction modifiers or anti-wear additives. Although this allows adsorption and reaction mechanisms to be elucidated, the systems are also greatly simplified and the influence of molecular structures, chain lengths and resulting interactions between the additive molecules cannot be taken into account. In the present study, we aimed at applying layers of a commercial friction modifier of different thickness to investigate the influence of the layer thickness on the film morphology and the friction behavior.

2. Materials

We used a commercially available nitrogen containing organic friction modifier, which is an organic compound whose chemistry is broadly described and the relevant physical properties given in [21]. The head group can be a propyl group, an ester group or an alcohol group.

Plate shaped samples are made of 99.5% pure iron(III) oxide (FE000414, GoodFellow GmbH, Hamburg, Germany). In order to achieve a reproducible surface quality, the plates are pre-processed on a semi-

automatic grinding and polishing machine (Buehler PowerPro 4000, Buehler ITW Test & Measurement GmbH, Esslingen a.N., Germany). For the grinding steps, a SiC paper (WS flex 18 C SK, Hermes Schleifmittel GmbH, Hamburg, Germany), with grit sizes 1200 (3 min, 35 N, rpm plate: 200), 2400 (3 min, 50 N, rpm plate: 200) and 4000 (2 x 2 min, 50 N, rpm plate: 150) is used. The coolant during the grinding steps is water. This is followed by two polishing steps on a polishing cloth (Microcloth SPT069 - PT Seda S, Cloeren Technology GmbH, Wegberg, Germany) with 3 µm and 1 µm monocrystalline diamond paste (DPA-M006 and DPA-M007, Cloeren Technology GmbH, Wegberg, Germany) (3 min each, 50 N, revolutions/min plate: 150). The coolant used during the polishing steps is ethanol-based (Lubricant Brown or Lubricant Blue, Cloeren Technology GmbH, Wegberg, Germany). The speed of the machine head is 150 rpm. Between each grinding and polishing step, the specimen holder and specimens are cleaned under running water to remove grinding particles. After separation of the specimens from the specimen holder, they are cleaned in an ultrasonic bath for 5 min each in acetone and then in isopropanol. The polished plates have an average roughness of R_A = 0.84 ± 0.33 µm. As counter body a diamond ball segment (Synton-MDP AG, Nidau, Schweiz) with a radius of 5.81 mm is used.

3. Methods

To determine the coefficient of friction without the influence of the ambient environment and the base oil, a tribometer in ultra-high vacuum (UHV) is used. The tribometer used in this work is a home-made design which is in more detail described on a publication by Marchetto et. al. [14]. The sample (an iron plate) sits on a sample plate, which in turn sits on a piezo actuator (stage). The actuator allows a highly precise movement of the specimen in x-, y- and z- direction (100 µm each). Control of the tribometer and data acquisition is made with LabView. The counter body is attached to a cantilever using superglue (UHU superglue, UHU GmbH, Brühl, Germany). In the friction test, the cantilever is deflected in the z-direction (normal force F_N) and in the y-direction (F_T), so that the coefficient of friction can be identified from the ratio. The deflection is determined with a laser interferometer. Two mirrors are placed direct at right angles to each other on the tip of the cantilever, directly above the counter body. Two incident laser beams (z- and y- direction) are reflected by the mirrors so that the deflection can be determined. Figure 1 shows the setup of the tribometer.

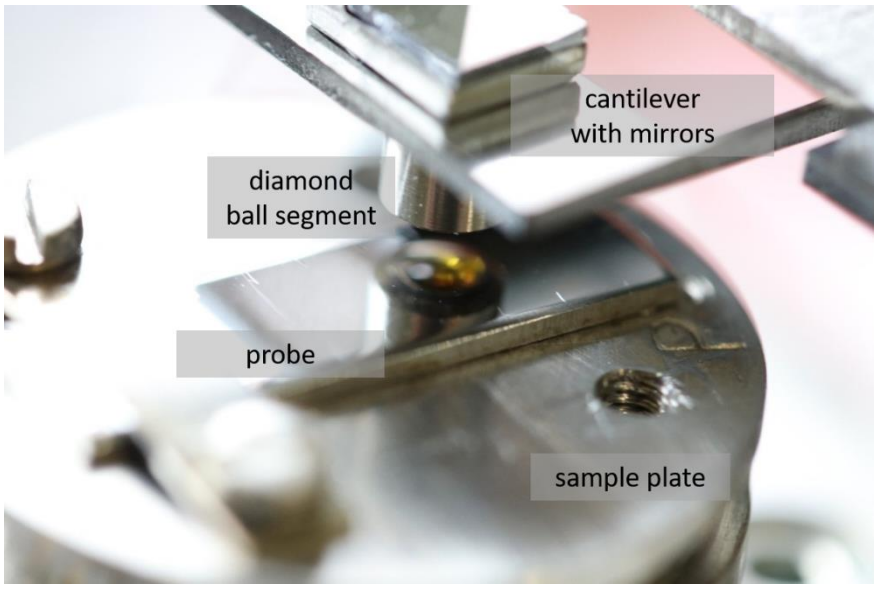

Figure 1 Setup of the UHV tribometer with an iron plate probe (mounted on sample plate) and a diamond ball segment as counter body (mounted on a cantilever with a mirror construction for measurements of the normal and transversal forces by interferometry)

The tribometer is connected to a vacuum transfer system so that the samples can be characterized before and after the friction tests using X-ray photoelectron spectrometry (XPS). The entire measurement setup is shown in Figure 2.

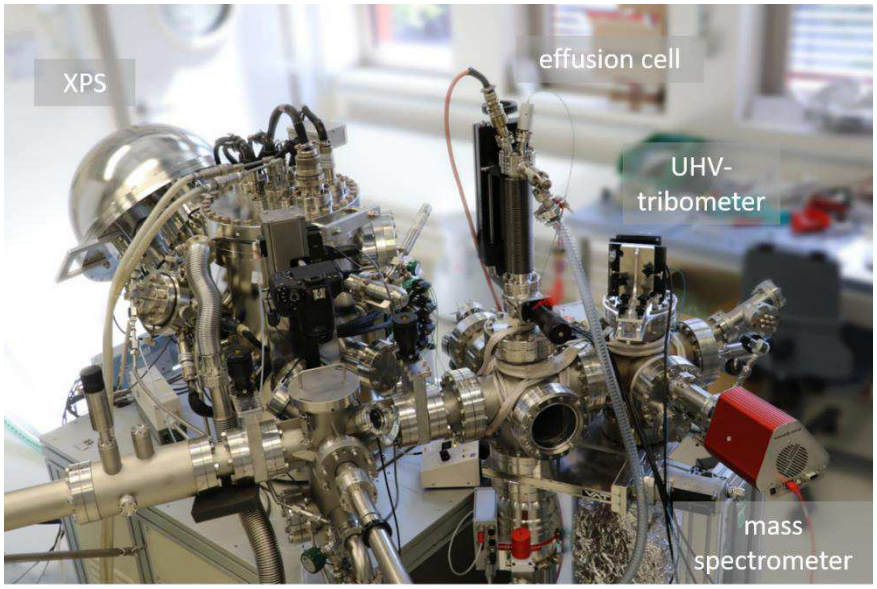

Figure 2 Measurement set-up at MikroTribologie Centrum µTC Karlsruhe with photoelectron spectrometer (XPS), effusion cell, tribometer and mass spectrometer

An effusion cell (Low Temperature Effusion Cell NTEZ, Dr. Eberl MBE-Komponenten GmbH, Weil der Stadt, Germany) is used to evaporate samples (here a friction modifier additive) for gas phase deposition. The effusion cell is integrated into the vacuum measurement system shown in Figure 2, so that the sample (i.e. the iron plate) can be cleaned in the XPS chamber by sputtering off the upper nanometers and then transferred into the effusion chamber without contact to atmosphere. Approximately 10 µg of the additive to be evaporated is brought into the effusion cell in a test tube made of quartz. The test tube is then heated electrically via a resistance heating wire by adjusting the voltage U and the current I. Once the evaporation temperature of the additive is reached, the vapor

plume leaves the evaporation cell before condensing on the sample. A mass spectrometer (PrismaPlus QMG 220, Pfeiffer Vakuum GmbH, Aßlar, Germany) is used to monitor the vapor pressure during the evaporation.

For chemical composition analysis, an X-ray photoelectron spectrometer (XPS), Versa Probe II (Physical Electronics, Inc. (PHI), Chanhassen MN, USA) is used. The spectrometer, operating in ultra high vacuum (< 10^{-6} mbar), is equipped with a monochromatic Al-Kα X-ray source (1486.6 eV) that achieves a minimum beam radius of 20 µm. The surface composition is measured with an XPS typical information depth < 5 nm. For overview spectra (0 - 1400 eV), pass energies of 187 eV are set in the hemisphere analyzer. In order to achieve a better resolution in detail spectra of the individual emission lines, the pass energy is lowered to 23 eV. The composition in atomic percent at.-% is calculated from the area integrals below the emission lines.

The steps of the experimental routine are described in more detail below.

After the samples have been introduced into the vacuum measurement system, they are cleaned from organic impurities by sputter cleaning in the XPS, which removes a maximum of 3 nm of the surface. For this purpose, the surface is sputtered in (5 × 5) mm² squares with 2kV and 2000 nA each. The sputter rate with this setting is calibrated to SiO_2 and amounts to approx. 2.5 nm/min. An overview spectrum is measured to confirm the cleaning step and to determine the composition of the initial surface.

For gas phase evaporation, the cleaned samples are transferred into the effusion chamber and kept outside the deposition radius of the effusion cell. The cell's temperature is controlled via a resistance heating and the temperature is raised stepwise by increasing the voltage to 4 V in 0.5 V/min steps. The current is reajusted accordingly. Through thermogravimetric analysis (TGA) of the friction modifier, it is known that the additive evaporates in 3 stages (supplementary information). At 134.9 °C, 18.5 % of the additive evaporates. The largest proportion of 77.9 % evaporates at 217.4 °C while at 353.3 °C a residue of 3.6 % still passes into the gas phase. Since the TGA measurement was performed at 1 Pa and the effusion cell operates in 4 - 5 orders of magnitude better vacuum, it can be assumed that evaporation already starts at lower temperatures. Figure 3 therefore shows a mass spectrum of the friction modifier during evaporation at about 235 °C.

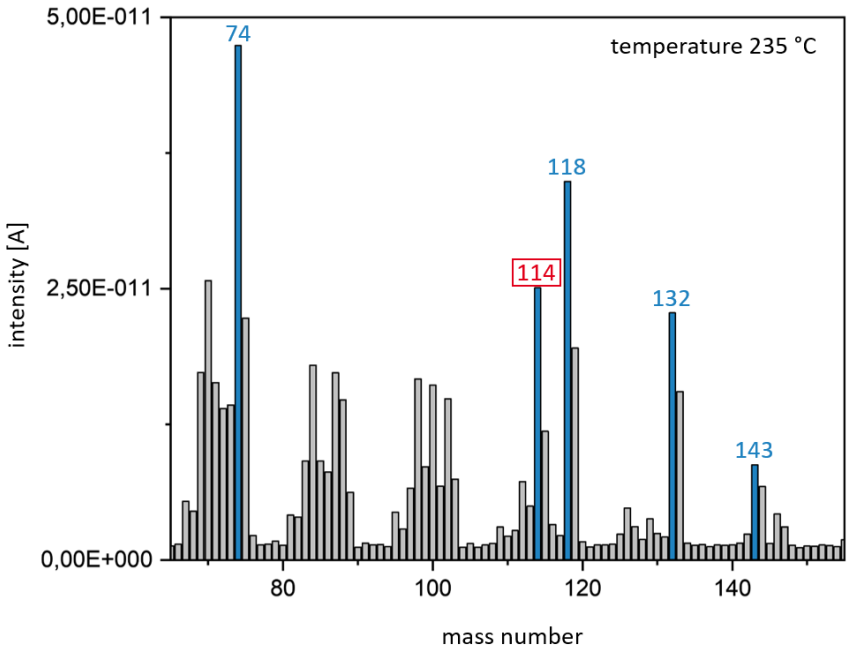

Figure 3 Intensities versus mass numbers during evaporation of the friction modifier at approx. 235 °C. The blue bars show the mass numbers 74, 114, 118, 132 and 143, which are characteristic for the friction modifier, while the gray bars represent background and other non-specific mass numbers. Mass number 114 (marked in red) represents the last evaporation stage.

Beginning at a temperature of about 235 °C, the intensity of mass number 114 increases. A temperature increase beyond that does not lead to an additional increase of the intensities, so that it can be assumed that at this temperature the entire additive is evaporated. Since all components of the additive are being deposited onto the iron plate, this mass number is used as an indicator. During the evaporation, for the sake of clarity only the partial pressures p_i of the individual components (p_{74}, p_{114}, p_{118}, p_{132} and p_{143}) are monitored over time. Once the partial pressure of mass number 114reaches the maximum, the sample is positioned at a distance of 10.6 cm centrally below the effusion cell. In order to determine the influence of the film thickness on the frictional behavior, the experiments are performed with a duration of 5 s, 30 s, 2 min, 4 min and 6 min. After the completion of the evaporation, the coated samples are then transferred to the tribo-chamber.

In the tribo-chamber, the coated specimen is positioned on the microtribometer stage. The normal force is set to 5 mN (average Hertzian pressure of 70 MPa). The sliding distance is set to 100 µm and speed is set to 50 µm/s. Each of the 222 cycles consist of a 100µm long outward and return path.

After the friction tests, the sample is transferred from the tribo-chamber back into the XPS chamber. Here, both an overview spectrum (0 - 1400 eV) and detail spectra of the emission lines of oxygen O1s, carbon C1s, nitrogen N1s and iron Fe2p are recorded. The measurements are performed in the area of the plate that appears dull in Figure 4. The area with the friction marks can be clearly seen in the center.

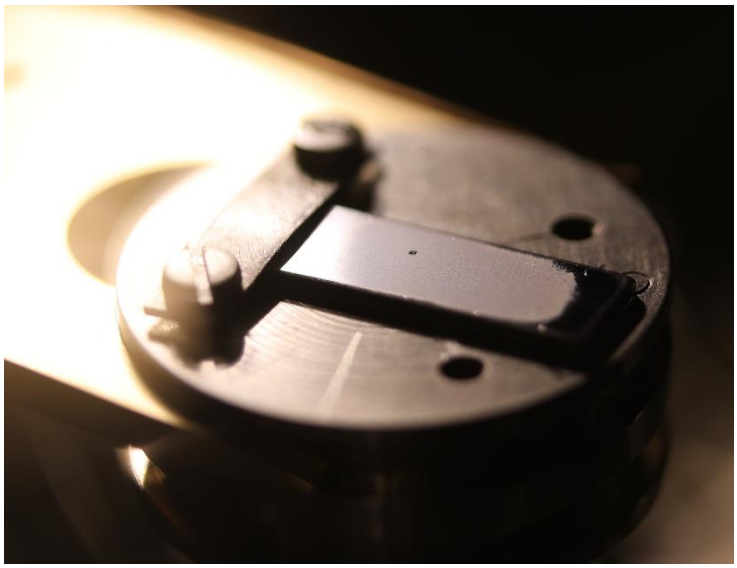

Figure 4 Sample carrier with iron plate after 4 min of gas deposition and a friction test. The dull area in the center of the plate is covered with the friction modifier; the friction marks are clearly visible in the center.

To see if the gas phase deposition is reversible, the surface is sputtered again in the area of the friction marks with the setting from the initial sputter cleaning (2 kV, 2000 nA, 5x5 mm²), following the surface analysis. For the samples, which were coated for 5 s and for 30 s this step is omitted.

Afterwards the samples are transferred to the tribo-chamber again to measure the friction force after sputtering. These subsequent friction tests are carried out with the same parameters mentioned above.

Finally, light microscope images and 3D topography images are taken of the surfaces and the friction tracks using a confocal microscope. These measurements are made outside the vacuum measurement system so that the surfaces are exposed to atmosphere.

4. Results

Gas phase deposition

Additives were deposited with different deposition times 5 s, 30 s, 2 min, 4 min and 6 min. The accompanying analysis with the mass spectrometer, as well as the prevailing pressures and temperatures is shown in the supplementary information.

The chemical composition of the iron plates after gas phase deposition was examined by XPS. Table 1 lists the results for the tests. After sputter cleaning (process step 1), the iron content (Fe) on the surface averages 40.7 at.%. Oxygen is present at an average of 57.1 at.%. Sputter cleaning can reduce the carbon content to an average of 2.2 at.%. The carbon content after gas deposition can thus be mostly assigned to the gas-deposited additive. After evaporation, the carbon content increases to 56.1 at.% (5 s), 73.7 at.% (30 S), 68.5 at.% (2 min), 65.5 at.% (4 min) and 65.7 at.% (6 min). The characteristic element for friction modifier, nitrogen N, is now present at the surface at 3.2 at.% (5 s), 2.9 at.% (30 s), 2.9 at.% (2 min), 4.5 at.% (4 min), and 7.7 at.% (6 min). The nitrogen content increases with longer deposition time, with the very short gas deposition time of 5 s being an exception here with 3.2 at.%. The iron and oxygen content decreases to an average of 6.4 at.% and 23.4 at.%, respectively, as a result of the deposition with friction modifier.

Table 1 Chemical composition of the iron plate surface after sputter cleaning (initial) and after evaporation (steamed) for the 5 s, 30 s, 2 min, 4 min, and 6 min experiments.

		Fe	O	C	N
		[at.-%]			
5 s	initial	52,8	43,7	3,5	0
	after deposition	9,1	31,6	56,1	3,2
30 s	initial	53,5	44,3	2,1	0
	after deposition	5,2	18,2	73,7	2,9
2 min	initial	30,7	68,4	0,9	0
	after deposition	5,2	23,3	68,5	2,9
4 min	initial	33,6	64,1	2,3	0
	after deposition	6,3	23,6	65,5	4,5
6 min	initial	32,7	64,9	2,4	0
	after deposition	6,4	20,3	65,7	7,7

Figure 5 shows the emission lines of oxygen O1s, carbon C1s, nitrogen N1s and iron Fe2p for the iron plate surface after the deposition for 2 min (red lines). Furthermore, the spectra for the initial surface (blue lines) and for the pure friction modifier (gray lines) are shown. The spectra for the substrate and friction modifier can be found in detail and with labels for the individual lines in the supplementary information and the raw data are given in [22]. The initial surface consists of iron oxides (Fe_2O_3) and a small amount of metallic iron. The metallic iron can either be detected below the thin oxide layer or the oxide layer is not continuous and metallic iron is exposed at some places. The friction modifier coating consists of various organic compounds consisting of carbon, oxygen and nitrogen, so that in addition to ether groups (C-O), carbonyls (C=O) and various amino compounds (NC_3, HNC_2, H_3N) are also detected. After gas phase deposition of the friction modifier on the initial surface, the emission lines for oxygen, carbon and nitrogen shift slightly in the direction of higher binding energies. There is no change in the chemical composition of the friction modifier. The emission lines of oxygen and iron (iron oxides) resulting from the substrate are still detectable after gas deposition, but the intensity decreases significantly.

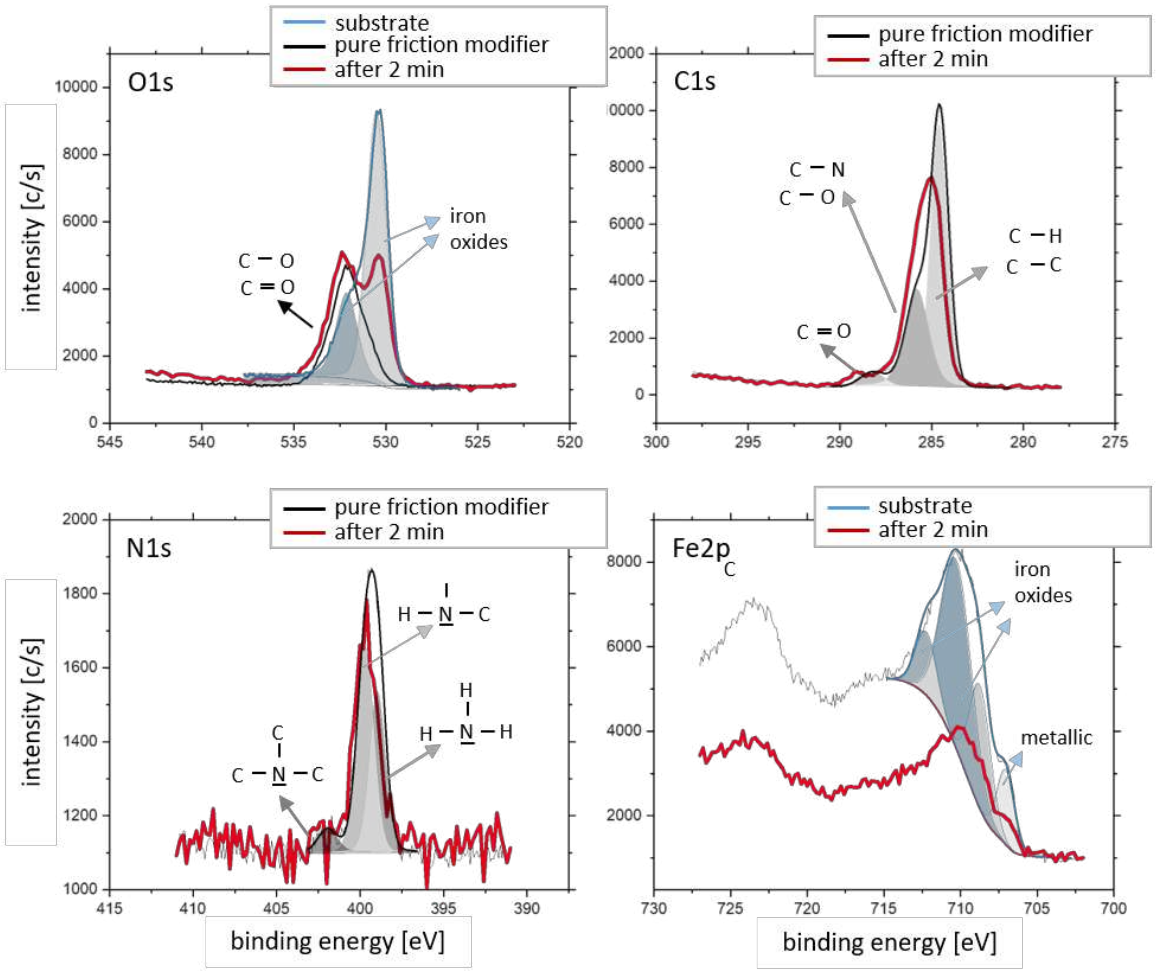

Figure 5 XPS high resolution spectra of the iron plate after 2 min evaporation with friction modifier (red lines) as well as the lines for the initial surface (blue lines) and the pure friction modifier friction modifier (gray lines), indication of the emission lines of oxygen O1s, carbon C1s, nitrogen N1s and iron Fe2p.

After the surface analysis of the coated plates, a 25 mm² area is sputtered in the area of the already existing friction marks (ablation < 3 nm, calibrated to SiO_2), in which further friction tests are subsequently carried out (see the following section). The chemical composition in the sputter spot can be taken from Table 2. The test with an evaporation time of 6 min was carried out with a new iron plate, so that the initial and the sputtered surfaces are compared.

After sputtering of the coated surface, iron is not detected anymore. The oxygen content is also reduced to 12.8 at.% on average. Both the carbon and nitrogen contents increase to an average of 81.9 at.% and 5.3 at.%, respectively. The corresponding spectra for the sample after a sputtering time of 2 min are shown in Figure 6. We notice that after sputtering, the chemical composition of the friction modifier does not change.

Table 2 Chemical composition of the iron plate surface after deposition and after sputtering (sputtered) for the 2 min, 4 min, and 6 min experiments.

		Fe	O	C	N
		[at.-%]			
2 min	after deposition	5,2	23,3	68,5	2,9
	sputtered	0	12,7	82,4	4,9
4 min	after deposition	6,3	23,6	65,5	4,5

	sputtered	0	12,7	81,5	5,9
6 min - 2	initial	28,5	70,6	0,9	0
	sputtered	0	13,1	81,8	5,1

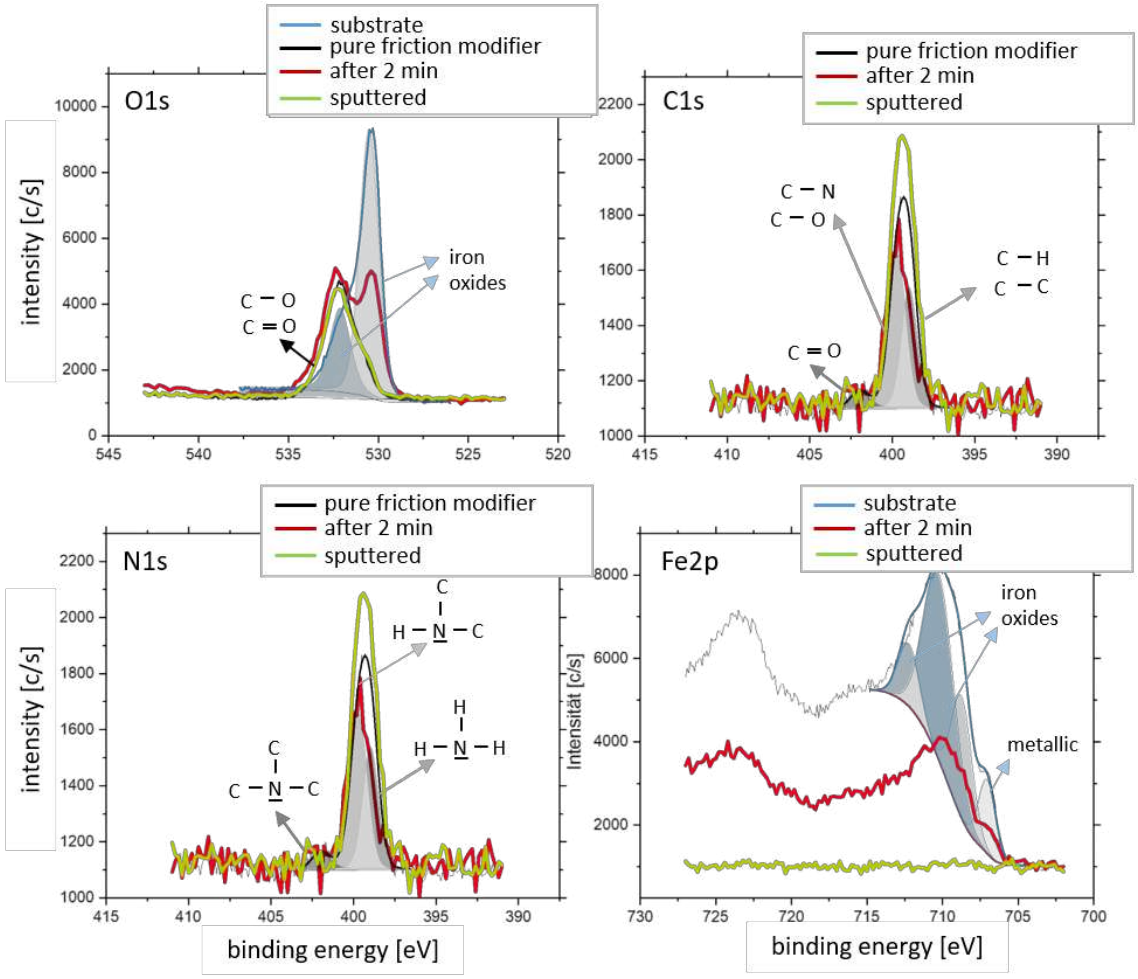

Figure 6 XPS high resolution spectra of the iron plate coated with for 2 min (red lines) and the subsequent sputtering step (green line) as well as the lines for the initial surface (blue lines) and the pure friction modifier (gray lines), indicating the emission lines of oxygen O1s, carbon C1s, nitrogen N1s, and iron Fe2p.

Figure 7 shows sections of the light microscopy images taken with the confocal microscope of the iron plate surfaces coated with friction modifier. The initial surface shows some fine grinding marks and some isolated surface defects or impurities (black spots). After 5 s of deposition, the grinding grooves of the initial surface are still visible and areas with an accumulation of small islands with a relatively uniform diameter of values < 0.05 µm appear. Since the larger black features are most likely the same defects or impurities that were observed for the initial surface, we can attribute that the islands are due to the adsorption of additive. After 30 s of deposition, the surface coverage with homogeneously distributed islands is almost complete. After 2 min, the diameter (approx. 1 µm) and height of islands have grown further. We used a Matlab code for circle detection to evaluate the droplet size and number. Since the island size corresponds approximately to the size of a pixel, the automatic circle detection cannot recognize them. However, the algorithm recognizes that these are modified areas which account for an area share of 11 %. After 4 min of evaporation, 27 % of the surface is covered with droplets, so that 79 droplets are present per (100 x 100) µm². The mean radius has further grown, presumably due to Ostwald ripening, to 3.2 ± 0.68 µm. The circle detection image and the

corresponding histogram are given in the supplementary information. For the longest evaporation time of 6 min, 2967 droplets are detected on the surface, covering 26 % of the area. The droplet density here is 97 droplets per (100 x 100) µm². The droplets have an average radius of 3.5 ± 0.79 µm. The images with the circle detection and the corresponding histograms are given in the supplementary information.

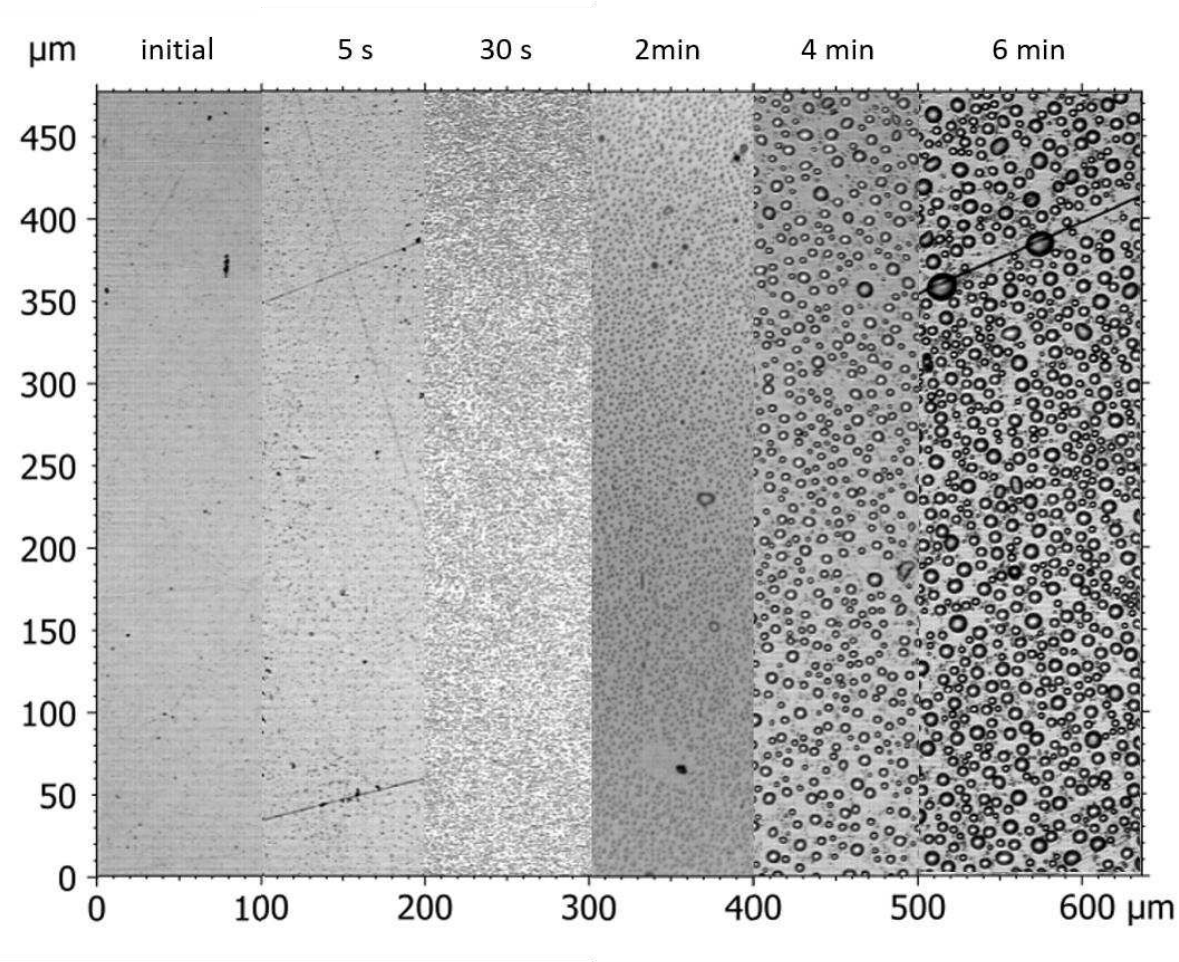

Figure 7 Gray images of the iron plate surfaces coated with friction modifier after 5 s, 30 s, 2 min, 4 min, and 6 min and the initial surface without gas deposition.

Friction

For comparison, we first describe the dry friction tests. The chemical composition of the surface for dry friction tests 1 and 2 corresponding to the average values of the initial surfaces are described in Table 1. In addition, small amounts of nitrogen and potassium were found on the surface (0.9 at.%), which can be attributed to contamination from the previous tests in the effusion chamber.

For each cycle, the friction force is recorded in forward and reverse sliding direction resulting in a lateral force loop. The mean value of the friction force F_R is divided by the mean normal force F_N of the respective friction test, so that the coefficient of friction COF is determined as the quotient. Each friction value determined in this way forms a data point. Since the tests are performed in a reversible motion, the piezo element accelerates or brakes near the reversal points. In order to consider only areas with constant velocity, all data points of the friction loops that are at a distance < 3 µm from the reversal points are not included in the mean value calculation. All raw data of the individual friction

tracks are given in [22]. The evaluation scheme is attached in the supplementary information on the basis of an example measurement.

The summarized results for the dry friction tests are plotted in Figure 8. During the dry friction test, the average normal force is 5.2 ± 0.7 mN. The average COF value was 0.19 ± 0.09 at the beginning of the test and continuously increased to 0.29 ± 0.22 by the end of the test. A trend cannot be identified with respect to the order of the individual friction tracks. With the exception of friction track 3, the friction values stabilize between 100 and 150 cycles. For the second dry friction experiment, the normal force of 5.7 ± 0.5 mN is around 0.5 mN higher than for the first dry friction experiment. At the start of the test, the average coefficient of friction is 0.13 ± 0.02. Over the first 25 cycles, the coefficient of friction then decreases (run-in) and then remains constant until approx. 120 cycles. After 120 cycles, the coefficient of friction increases significantly for all individual friction tracks, so that at the end it is 0.51 ± 0.02 on average. The slope increases with ascending order of the individual friction tracks.

The dry friction track 3 is measured on a surface with an increased proportion of metallic iron. For this purpose, the initial surface (iron oxide with organic impurities) is removed by sputtering off 30 nm so that 72.6 at.% iron and 26.8 at.% oxygen are still present on the surface. The evaluation of the Fe2p line shows that it is 57.57 at.% metallic and 42.43 at.% oxidic iron (supplementary information). For the dry friction test 3, the normal force is 5.5 ± 0.4 mN. The progression of the friction coefficients is similar for all friction tracks. At the beginning, it averages 0.21 ± 0.001 and then increases to 2.4 ± 0.4 with a depressive progression. Here the friction jumps steeply at about 150 cycles and the friction coefficient rises into the triple-digit range. Since the cantilever spring does not permit such high forces, this is most presumably a measurement error, so that the corresponding data is excluded from the mean value calculation from 150 cycles onwards.

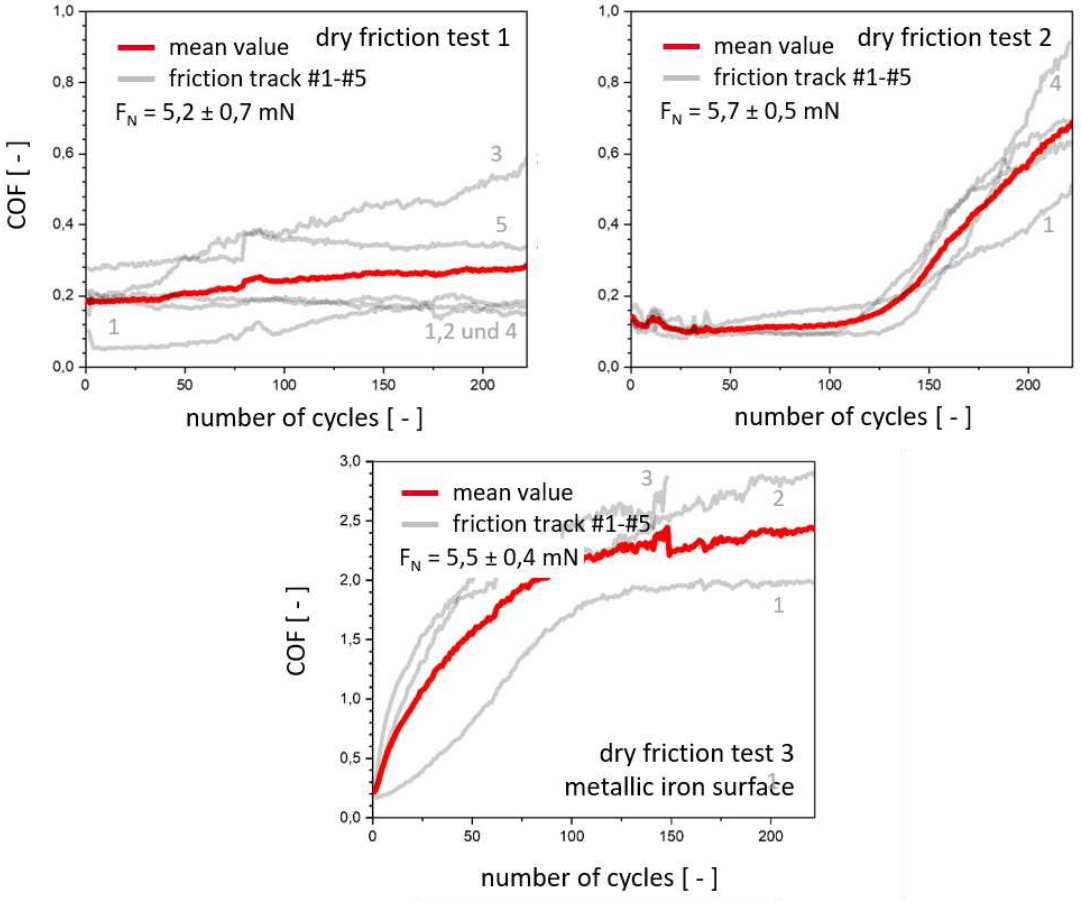

Figure 8 Coefficient of friction versus number of cycles for the UHV tribometer tests for dry friction, counterbody diamond ball, nominal normal force FN = 5 mN (corresponds to a mean Hertzian pressure of 70 MPa), number of cycles N = 222, velocity v = 50 µm/s (reversing), gray curves: single friction tracks (partially numbered), red curves: same mean value of the single friction tracks

The friction tests on the iron plates coated with friction modifier are shown in Figure 9. For the shortest deposition time of 5 s, the friction coefficient is constant at a level of 0.06 to 0.05. Friction track 1 shows the highest friction coefficient, while the friction coefficients of friction track 2 and 3 are at a similar but lower level. For 30 s evaporation duration, the average friction value at the beginning is 0.04 ± 0.01. After approx. 50 cycles, the friction value for friction track 1 and 2 starts to increase. The coefficient of friction of friction track 3 remains constant. The average coefficient of friction at the end of the test is 0.07 ± 0.02. For the deposition duration of 2 min, the average coefficient of friction decreases from 0.1 ± 0.02 to 0.07 ± 0.01 over the first 25 cycles. After 25 cycles, the friction value increases again. For friction tracks 1 and 3, the coefficient of friction reaches a maximum between 100 and 150 cycles before decreasing again. The coefficient of friction track 2 does not increase as much, decreases again after 75 cycles and then remains constant from cycle 100. At the end of the test, the average coefficient of friction is 0.11 ± 0.04. The average normal force for the test is 5.4 ± 0.3 mN. For the friction tests on the iron plate coated for 4 min, the normal force is 5.4 ± 0.4 mN. The friction coefficient decreases from 0.16 ± 0.02 to 0.07 ± 0.01 on the first 50 cycles and then increases to 0.09 ± 0,001 by the end of the experiment. Friction track 3 shows an non-plausible jump at cycle 170 and is therefore no longer taken into account for the mean value calculation. After an evaporation duration of 6 min, the friction value decreases continuously from an initial average of 0.09 ± 0.02 to 0.06 ± 0.02.

Friction track 1 shows the highest friction value and the most unstable course compared to friction track 2 and 3. The normal force for this test was 5.7 ± 0.5 mN.

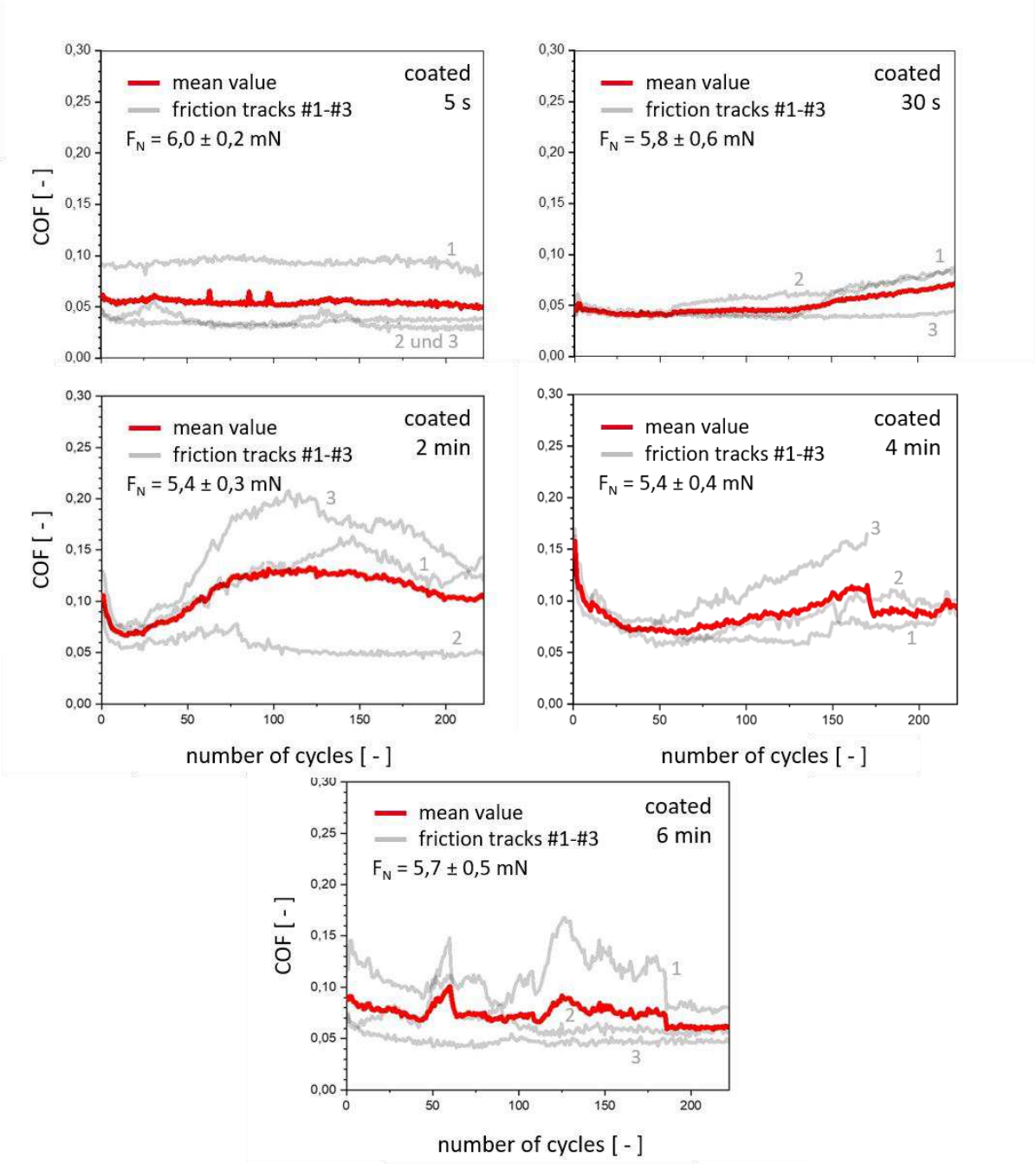

Figure 9 Coefficient of friction versus number of cycles for the UHV tribometer tests on the iron plates coated with friction modifier, gasization duration: 5 s, 30 s, 2 min, 4 min and 6 min, counterbody diamond sphere, nominal - normal force FN = 5 mN (corresponding to a mean Hertzian pressure of 70 MPa), number of cycles N = 222, velocity v = 50 µm/s (reverberating), gray curves: individual friction tracks (with indication of sequence), red curves: moving average of individual friction tracks

Figure 10 shows the friction coefficient curves for the tests on the coated and subsequently sputtered surfaces. The friction tests are carried out on the sputtered area. The tests on the 2 min deposited plates are carried out with a normal force of 5.5 ± 0.5 mN. The coefficient of friction decreases from 0.17 ± 0.02 on the first 25 cycles to 0.08 ± 0.01 and then remains stable, so that the coefficient of friction averages 0.09 ± 0.03 at the end. In the sputtered area after the deposition for 4 min, the coefficient of friction decreases from 0.13 ± 0.01 to 0.07 ± 0.00 on the first 50 cycles and then remains

stable. No run-in is observed for the test after 6 min deposition time. The coefficient of friction decreases continuously from 0.11 ± 0.02 to 0.07 ± 0.02. The normal force was 5.8 ± 0.7 mN.

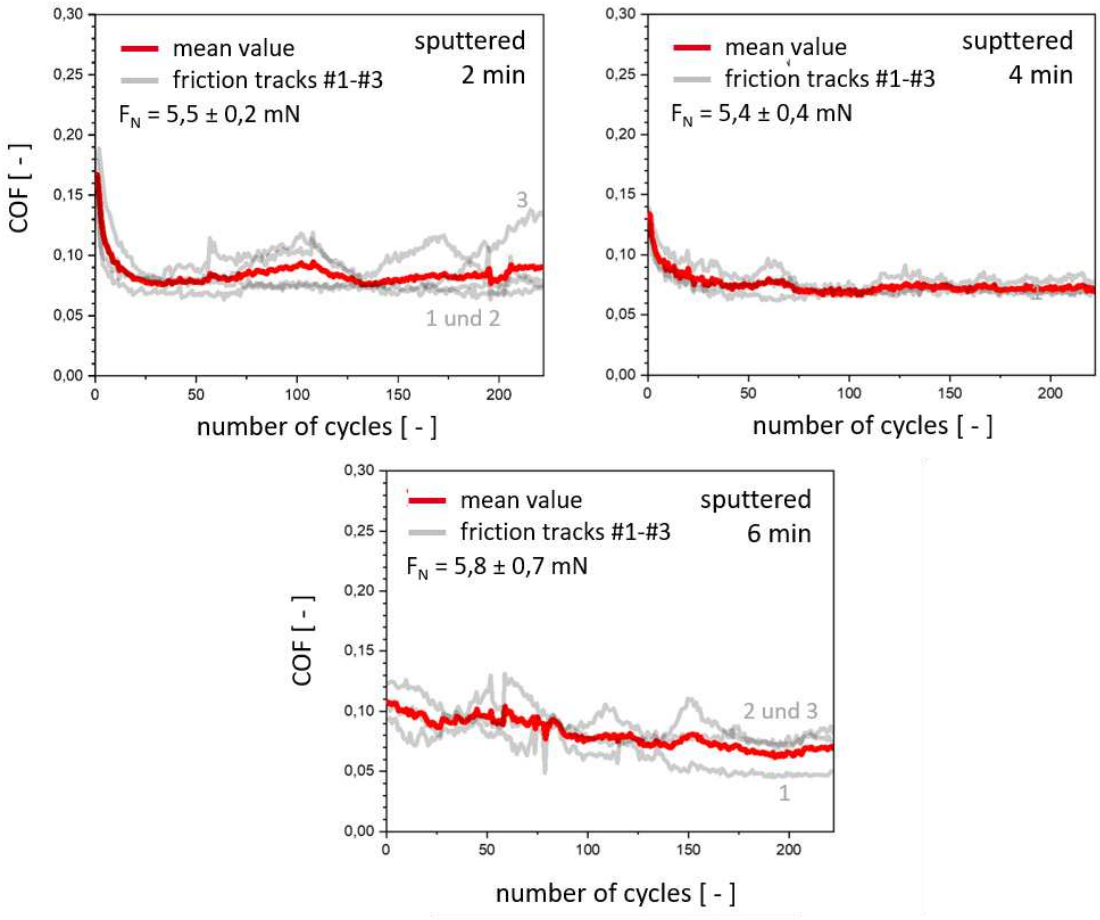

Figure 10 Coefficient of friction versus number of cycles for the UHV tribometer tests on the iron plates coated with friction modifer followed by sputtering, ablation < 3 nm (friction traces in the sputter spot), vapor deposition duration: 2 min, 4 min and 6 min, counterbody diamond sphere, nominal - normal force FN = 5 mN (corresponding to a mean Hertzian pressure of 70 MPa), number of cycles N = 222, velocity v = 50 µm/s (reversing), gray curves: single friction marks (partially numbered), red curves: moving average of single friction marks.

Following the friction tests on the coated specimens, the friction marks are clearly visible. They are located in the center of an approximately circular recess in the otherwise droplet-covered plate surface. This effect is most clearly seen on the sample that was coated for 6 min (see Figure 11). A large elongated droplet spreads out over 3 friction tracks. The topography image depicted in Figure 11, shows that the friction tracks represent wear scars up to 1 µm. The same effect can be observed for the other evaporation durations.

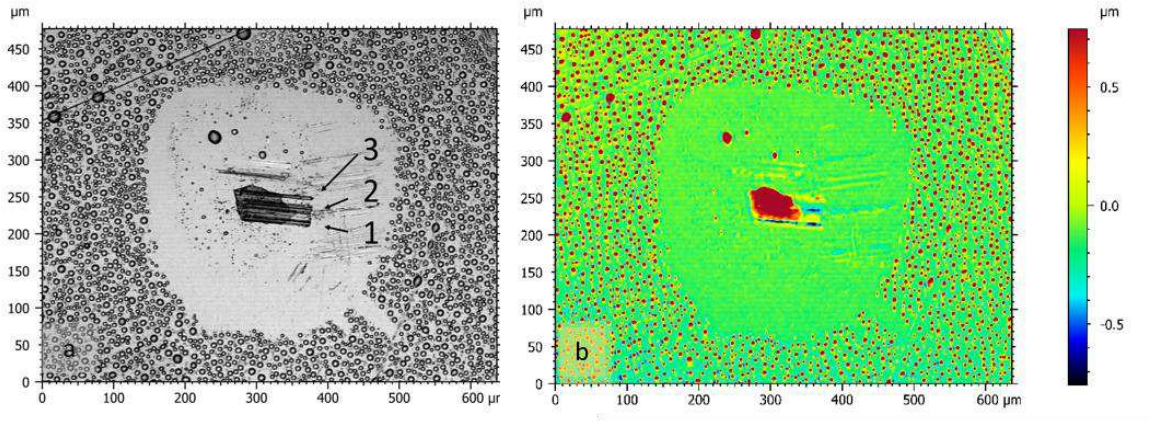

Figure 11 Gray image (a) and topography image (b) of the ironplatet surfaces after the friction tests after 6 min of evaporation time with friction modifier (counterbody diamond sphere, nominal normal force FN = 5 mN (corresponding to a mean Hertzian pressure of 70 MPa), number of cycles N = 222, velocity v = 50 µm/s (reversing)).

Discussion

The gas phase lubrication experiments aimed at applying layers of a commercial friction modifier of different thickness in order to investigate the influence of the layer thickness on the friction behavior. In the first step, iron plates with a native oxide layer were coated with friction modifier using an effusion cell. The gas phase deposition was successfully carried out for deposition durations of 5 s, 30 s, 2 min, 4 min and 6 min. Surface chemical analysis show that gas phase deposition decreases the iron content from 30.7 % (initial) to 5.2 - 6.4 at.%. In contrast, the content of nitrogen, which can be regarded as a marker for the friction modifier, increases to 3.2 at.% (5 s), 2.9 at.% (30 s and 2 min), 4.5 at.% (4 min) and 7.7 at.% (6 min). With increasing deposition durations, the content of nitrogen also increased. The XPS spectra show that the chemical composition of the additive does not change as a result of evaporation and condensation on the surface (see Figure 5)

Ex-situ images of the coated surfaces taken with a confocal microscope show that the additive adsorbs with a droplet-shaped morphology using vapor deposition (see Figure 7). To the best of our knowledge, this morphology has not been found previously in other gas phase lubrication studies to date (e.g. [12, 15–18]) using other friction modifier additives. The morphology is also not consistent with the previously reported ‘thick film’ lubrication that has been seen in interferometry studies [11].

For the shortest deposition time, structures cannot be detected yet. After 30 s, the surface appears marbled in light microscopy images, and after 2 min, clearly punctiform structures can be recognized. An analysis of the droplet size showed radii of about 1 µm (graphically estimated) for 2 min, 3.2 ± 0.68 µm on average for 4 min and 3.5 ± 0.79 µm on averaged for 6 min. With the aid of automatic circle detection, a surface coverage of 27 % (79 droplets per (100 x 100) µm²) was determined for the surface after 4 min of evaporation and a surface coverage of 26 % (97 droplets per (100 x 100) µm²) after 6 min of evaporation. Strictly, it is not possible to discuss the influence of the layer thickness on the friction behavior, but the influence of the droplet height and distribution. However the droplet height cannot be precisely determined through the radius, since the droplets are so large that the gravitational force has an influence [23].

For the deposition times 2 min, 4 min and 6 min, the surfaces covered with droplets were sputtered afterwards. Sputtering alters the droplet morphology so that a continuous film is formed on the surface. The detailed spectra of the XPS show no chemical changes due to this step. Only the very small

measured intensity of the iron emission line indicates that a continuous additive film has formed. Assuming that this film is homogeneous, a film thickness d can be determined using formula 1:

$$d = \lambda_{sub} cos\theta \ln\left(\frac{I_{sub}}{I_0}\right) \quad (1)$$

Here, I_0 describes the intensity of the elements initially present in the substrate, I_{sub} the intensity of the elements after coating, λ_{sub} the mean free path length in the substrate and θ the acceptance angle of the XPS, typically 45 °. The film thicknesses determined in this way are 0.96 nm (2 min), 1.4 nm (4 min) and 1.55 nm (6 min) and thus become thicker with increasing evaporation times, corresponding to the larger and more numerous droplets.

In order to discuss the friction behavior, it is necessary to point out a phenomenon that is also very interesting. In the image of the surface coated for 6 min and after the tribo test, a roughly circular droplet-free area measuring approx. 350 µm in diameter can be seen (see Figure 11). Otherwise, on the friction tracks an accumulation of liquid can be seen. We ascribe this observation to capillary interactions, that occured between the diamond counterbody and the droplets. The evaluation of a force-time curve during the approach of the sphere to the coated surface shows an attractive interaction (supplementary information) and thus confirms the assumption. Unfortunately, the distance at which the attractive interaction begins, cannot be determined from the recorded curves. This information would give an indication of the actual droplet height. However, the real droplet height can be calculated with simple geometric considerations (see supplementary information):

$$h_{\mathrm{real}} = r - \sqrt{r^2 - \left(\frac{d_{real} - s}{2}\right)^2} \quad (2)$$

For an evaporation time of 6 min, formula 2 gives a real droplet height of 1.34 µm. The ratio of height to radius for the friction modifier droplets in vacuum is 0.38. The droplet height after an evaporation time of 2 min is 0.38 µm and after 4 min 1.2 µm.

Figure 12 shows the box plots of the friction coefficients for the tests on the coated iron plate surfaces after 5 s, 30 s, 2 min, 4 min, 6 min and for dry friction. Within the box are half of the measured values and the error bars indicate the standard deviation. In addition, the median line, the mean value and outliers are shown. Figure 12, left shows the mean values of the friction coefficients over cycles 1 to 222 and this includes all ranges of the friction coefficient curves such as run-in, stabilization phase and possible lubrication failure. Figure 12, right, shows the friction coefficient at the end of the friction test, for the 222nd cycle. The friction coefficient for dry friction, which summarizes the results of dry friction test 1 and 2, is the highest, both for the mean value (0.244) and at the end (0.465). Dry friction test 3 on increased metallic iron content is not included in the calculation, as the surface is not comparable here. The smallest friction coefficients are found for the evaporation durations of 5 s and 30 s. After 5 s, the mean value of the friction coefficient is 0.054 and at the end 0.05. After 30 s, the mean value of the friction coefficient is at the same level at 0.05 and at the end slightly higher at 0.074. The friction tests on the plates coated for 2 min have the highest friction coefficient both at the mean (0.109) and

at the end (0.104). For the 4 min and 6 min deposition durations, the coefficients of friction then decrease again to 0.088 and 0.074 on average and 0.093 and 0.061 at the end.

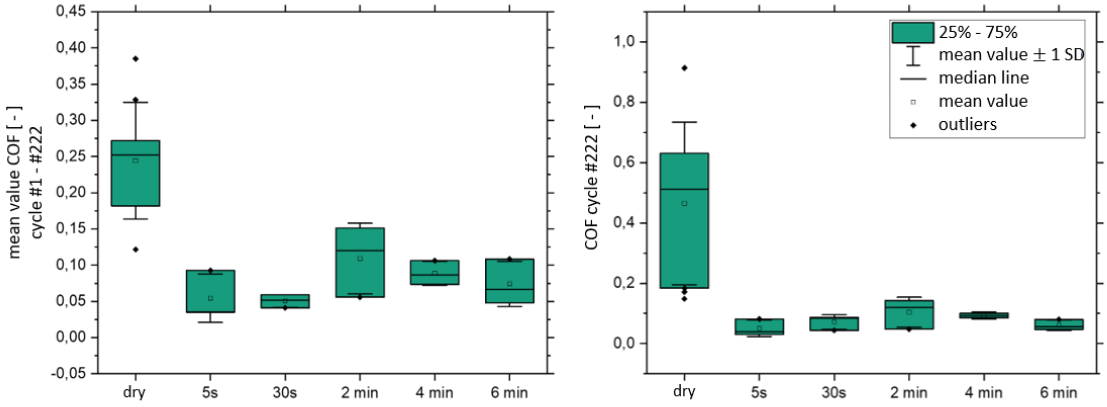

Figure 12 Boxplot of the friction values for the tests on the coated iron plate surfaces after 5 s, 30 s, 2 min, 4 min, 6 min and for dry friction (counterbody diamond ball, nominal normal force FN = 5 mN, mean Hertzian pressure = 70 MPa), left: mean value of the friction coefficient over all cycles (1-222), right: friction coefficient at cycle 222. Half of the measured values lie within the box, the error bars indicate the standard deviation. In addition, the median line, the mean value and the outliers are shown.

The trend within the tests with gas phase deposited friction modifier is explained on the basis of the droplet size and the associated capillary effect. Figure 13 shows the friction force curve over the friction distance (0 - 100 µm) of the first friction cycle. On these 100 µm, the droplets which have not already coalesced due to the approach of the diamond ball in the gap and form a large "droplet" are collected. The friction forces for the dry test, as well as for the short evaporation durations of 5 s and 30 s, are at a similar level around 0.4 mN. Interestingly, the curve of the experiment after 6 min of evaporation is also at this level. The tests after 2 min and 4 min of evaporation both show a clear increase in the frictional force on the first 10 µm of the friction path, so that values of 1 mN and 1.15 mN are reached at the end of the path at 100 µm.

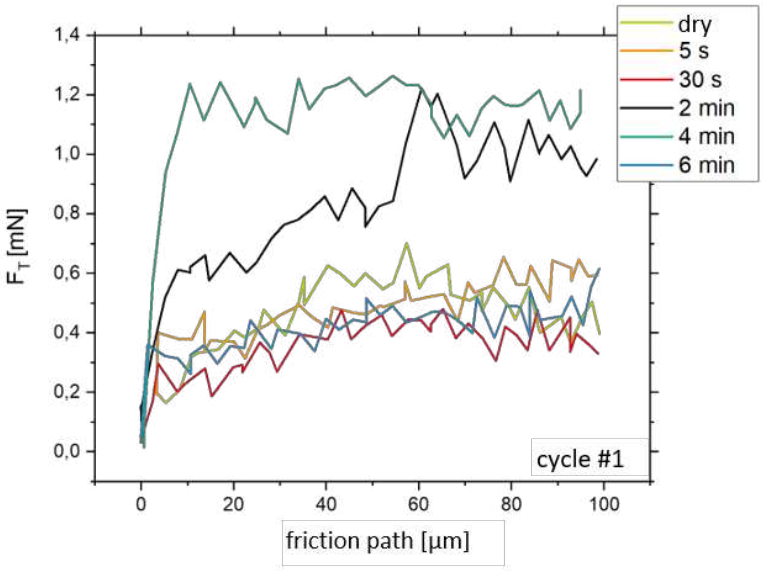

Figure 13 Friction force F_T over the friction path in cycle 1 for the experiments on the coated iron plate surfaces after 5 s, 30 s, 2 min, 4 min and 6 min and for the experiment dry friction 1 (counterbody diamond sphere, nominal normal force FN = 5 mN, mean Hertzian pressure = 70 MPa)

The additional frictional force that has to be applied here is attributed to the capillary forces acting. The diamond ball experiences not only the actual frictional force, but also the resistance due to the droplet and the associated force that must be applied to pull it along in the friction gap. It can be assumed that after 6 min of evaporation, the droplet is so large and thus the volume in the friction gap is fully filled so that it no longer moves. This condition would correspond to friction in liquid. The additional force F_C to be applied can be determined from the difference between the friction force of the tests without capillary effect $F_{C,without}$ and with capillary effect $F_{C,with}$. For the levels of $F_{C,without}$ and $F_{C,with}$, values of 0.48 mN and 1.08 mN result, and thus a resulting capillary force F_K of. 0.595 mN.

The plot of the mean friction coefficients versus droplet height (0.34 µm after 2 min, 1.2 µm after 4 min and 1.34 µm after 6 min) is shown in Figure 14. Under the hypothesis that there is a critical droplet radius at which the friction coefficient starts to decrease again, a parabola can be fitted to the data (R-squared = 0.97863, N = 5). Very small values are assumed for the droplet heights after 5 s and 30 s (0.01 µm and 0.02 µm). The critical droplet radius is thus 0.73 µm. Due to the limited data available, this value cannot be regarded as certain, but as plausible as a guide value. Since liquid friction can be assumed from an evaporation time of 6 min (possibly even earlier), the coefficient of friction should not decrease further for larger droplet radii.

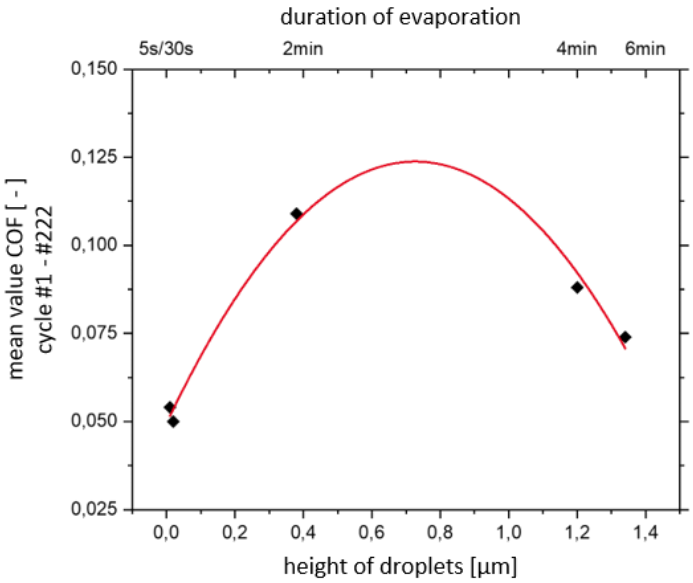

Figure 14 Mean value of friction coefficient over all cycles (1-222) versus droplet height of the gasized ironplatets after 5 s, 30 s, 2 min, 4 min, and 6 min; red line corresponds to the parabolic fit function $f(x)=a+bx+cx^2$ with parameters a = 0.05 ± 0.004, b = 0.204 ± 0.022, and a = 0.0163 ± 0.016 (R-squared = 0.97863, N = 5).

If the surface covered with droplets is sputtered for a short time, a continuous layer of chemically unmodified friction modifier is formed. The layer thicknesses are 0.96 nm (2 min), 1.4 nm (4 min) and 1.55 nm (6 min). The decreasing trend for longer vapor deposition times can also be observed for the friction tests on the sputtered surfaces (see Figure 15). The highest mean friction value of 0.09 and at the end of 0.085 is found for the 2 min deposition and then sputtered surface. The friction value for the 4 min surface is 0.072 on average and 0.075 at the end. The measured coefficients of friction for the sputtered surfaces lower than the corresponding coefficients of friction on the droplets as the capillary force is reduced. Only for the 6 min coated sample, the coefficient of friction is higher after sputtering than on the droplets. It is 0.069 on average and 0.081 at the end of the friction test. In addition, the trend shows that the scatter of the friction values for the sputtered surfaces is smaller than for the friction values determined on the surfaces covered with droplets. If the friction value is plotted as a function of the coating thickness after sputtering, the coefficient follows a linear relationship (see Figure 16). Since we have observed that the droplets accumulate under the spherical counter surface, it is reasonable to speculate that the friction modifier will form similar thick films in lubricated contact when the additive is subjected to high shear and as a result loses the droplet shaped morphology. The presented experimental strategy therefore allows systematic studies of the friction modifiers' film thickness without having to deal with hydrodynamic effects that change the lubricant film thickness.

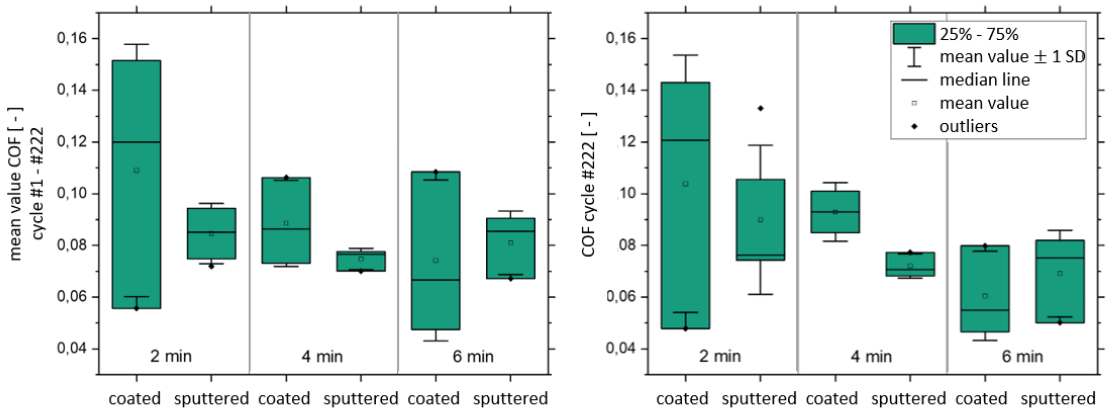

Figure 15 Boxplot of the friction values for the tests on the coated and afterwards sputtered iron plate surfaces after 2 min, 4 min, 6 min (counterbody diamond ball, nominal normal force FN = 5 mN, mean Hertzian pressure = 70 MPa), left: mean value of the friction coefficient over all cycles (1-222), right: friction coefficient at cycle 222. Half of the measured values lie within the box, the error bars indicate the standard deviation. In addition, the median line, the mean value and the outliers are shown.

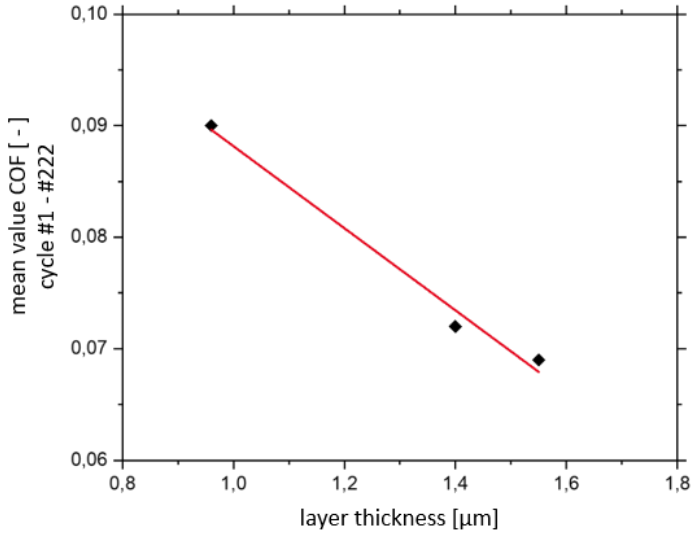

Figure 16 Mean value of the coefficient of friction over all cycles (1-222) versus layer thickness of the coated and afterwards sputtered iron plate surfaces after 2 min, 4 min, and 6 min; red line corresponds to the linear fit function f(x)=a+bx with parameters a = 0.125 ± 0.006 and b = -0.037 ± 0.004 (Pearson-R = -0.99344, N = 3).

Conclusion

By combining an effusion cell, a tribometer and a XPS in a vacuum measuring system, it was possible to deposit a technical friction modifier to a defined iron oxide surface and to study the morphology as well as the frictional behavior without the influence of the base oil. In this environment, the additive forms droplets whose radii and heights increase with increasing deposition time. In friction tests, low friction values were observed for small and for large droplets. In between, there are critical droplet sizes at which capillary effects occur which increase the coefficient of friction. This particular behavior id expect to the correlation between droplet height and friction properties and should be further investigated with regard to the critical droplet height. For this purpose, tests with evaporation durations between 2 min and 4 min are necessary. Furthermore, with evaporation durations > 6 min,

it can be investigated whether the coefficient of friction decreases further or actually remains constant as assumed. Subsequently, the findings obtained in vacuum are to be confirmed with experiments under lubricating conditions.

Declarations

Funding:
Not applicable

Conflicts of interest/Competing interests:
The authors declare that they have no known competing financial interests or personal relationships that could have appeared to influence the work reported in this paper

Availability of data and material:
https://fordatis.fraunhofer.de/handle/fordatis/206
http://dx.doi.org/10.24406/fordatis/133

Code availability:
Not applicable

Literatur

[1] H. Spikes, *Tribol Lett* **2015**, *60 (1)*, 119 – 145. DOI: 10.1007/s11249-015-0589-z.

[2] Z. Tang, S. Li, *Current Opinion in Solid State and Materials Science* **2014**, *18 (3)*, 119 – 139. DOI: 10.1016/j.cossms.2014.02.002.

[3] F. P. Bowden, J. N. Gregory, D. Tabor, *Nature* **1945**, *156 (3952)*, 97 – 101. DOI: 10.1038/156097a0.

[4] S. G. Daniel, *Trans. Faraday Soc.* **1951**, *47 (0)*, 1345 – 1359. DOI: 10.1039/TF9514701345.

[5] S. Loehle, C. Matta, C. Minfray, T. Le Mogne, J.-M. Martin, R. Iovine, Y. Obara, R. Miura, A. Miyamoto, *Tribology Letters* **2014**, *53 (1)*, 319 – 328. DOI: 10.1007/s11249-013-0270-3.

[6] S. Campen, J. H. Green, G. D. Lamb, H. A. Spikes, *Tribol Lett* **2015**, *57 (2)*, 51-71. DOI: 10.1007/s11249-015-0465-x.

[7] S. Bernat, S. Armada, N. Espallargas, *Tribol Lett* **2018**, *66 (3)*, 83. DOI: 10.1007/s11249-018-1035-9.

[8] T. Kuwahara, P. A. Romero, S. Makowski, V. Weihnacht, G. Moras, M. Moseler, *Nature Communications* **2019**, *10 (1)*, 151. DOI: 10.1038/s41467-018-08042-8.

[9] W. B. Hardy, I. Doubleday, *Proceedings of the Royal Society of London. Series A, Containing Papers of a Mathematical and Physical Character* **1922**, *100 (707)*, 550 – 574. DOI: 10.1098/rspa.1922.0017.

[10] M. Ratoi, V. Anghel, C. Bovington, H. Spikes, *Tribology International* **2000**, *33 (3-4)*, 241 – 247. DOI: 10.1016/S0301-679X(00)00037-2.

[11] V. Anghel, C. Bovington, H. A. Spikes, *Lubr. Sci.* **1999**, *11 (4)*, 313 – 335. DOI: 10.1002/ls.3010110402.

[12] M.-I. de Barros Bouchet, J.-M. Martin, in *Advanced Analytical Methods in Tribology* (Eds: M. Dienwiebel, M.-I. de Barros Bouchet), Springer International Publishing. Cham **2018**.

[13] J.-M. Martin, T. Le Mogne, C. Grossiord, T. Palermo, *Tribology Letters* **1997**, *3 (1)*, 87 – 94. DOI: 10.1023/A:1019183711497.

[14] D. Marchetto, R. Benzig, S. Korres, M. Dienwiebel, *Tribology - Materials, Surfaces & Interfaces* **2012**, *6 (3)*, 95 – 101. DOI: 10.1179/1751584X12Y.0000000012.

[15] D. Philippon, M.-I. de Barros-Bouchet, T. L. Mogne, E. Gresser, J.-M. Martin, *Tribology - Materials, Surfaces & Interfaces* **2007**, *1 (3)*, 113 – 123. DOI: 10.1179/175158408X273586.

[16] D. Philippon, M.-I. de Barros-Bouchet, O. Lerasle, T. Le Mogne, J.-M. Martin, *Tribology Letters* **2011**, *41 (1)*, 73 – 82. DOI: 10.1007/s11249-010-9685-2.

[17] D. Philippon, M.-I. de Barros-Bouchet, T. Le Mogne, O. Lerasle, A. Bouffet, J.-M. Martin, *Tribology International* **2011**, *44 (6)*, 684 – 691. DOI: 10.1016/j.triboint.2009.12.014.

[18] M. C. Righi, S. Loehlé, M.-I. de Barros Bouchet, D. Philippon, J.-M. Martin, *RSC Adv* **2015**, *5 (122)*, 101162 – 101168. DOI: 10.1039/C5RA14446A.

[19] R. Rana, W. Tysoe, *Tribology Letters* **2019**, *67 (3)*, 93. DOI: 10.1007/s11249-019-1205-4.

[20] J. Martin, T. Le Mogne, M. Boehm, C. Grossiord, *Tribology International* **1999**, *32 (11)*, 617 – 626. DOI: 10.1016/S0301-679X(99)00090-0.

[21] A. K. Jung, L. Voelkel, S. Crema, *EP 2321389B1*.

[22] J. Eickworth, J. Wagner, P. Daum, *Raw Data: Gas phase lubrication study with an organic friction modifier; http://dx.doi.org/10.24406/fordatis/133*.

[23] F. Mugele, J. Heikenfeld, in *Electrowetting*, John Wiley & Sons, Ltd **2018**.

Supplementary Files

This is a list of supplementary files associated with this preprint. Click to download.

- SupplementaryInformationfinal.pdf